

Continuum bound states K_L , $D_1(2420)$, $D_{s1}(2536)$, and their partners K_S , $D_1(2400)$, $D_{sJ}^*(2463)$

Eef van Beveren

Centro de Física Teórica

Departamento de Física, Universidade de Coimbra

P-3000 Coimbra, Portugal

eef@teor.fis.uc.pt

George Rupp

Centro de Física das Interações Fundamentais

Instituto Superior Técnico, Edifício Ciência

P-1049-001 Lisboa Codex, Portugal

george@ajax.ist.utl.pt

PACS number(s): 12.40.Yx, 14.40.Aq, 14.40.Lb, 13.25.Es, 13.25.Ft, 13.75.Lb

November 8, 2018

Abstract

The very recently observed $D_{sJ}^*(2463)$ meson is described as a $J^P = 1^+ c\bar{s}$ bound state in a unitarised meson model, owing its existence to the strong OZI-allowed 3P_0 coupling to the nearby S -wave D^*K threshold. By the same non-perturbative mechanism, the narrow axial-vector $D_{s1}(2536)$ resonance shows up as a quasi-bound-state partner embedded in the D^*K continuum. With the same model and parameters, it is also shown that the preliminary broad $1^+ D_1(2400)$ resonance and the established narrow $1^+ D_1(2420)$ may be similar $c\bar{n}$ partners, as a result of the strong OZI-allowed 3P_0 coupling to the nearby S -wave $D^*\pi$ threshold. The continuum bound states $D_1(2420)$ and $D_{s1}(2536)$ are found to be mixtures of 33% 3P_1 and 67% 1P_1 , whereas their partners $D_1(2400)$ and $D_{sJ}^*(2463)$ have more or less the opposite $^{2S+1}P_1$ -state content, but additionally with some $D^*\pi$ or D^*K admixture, respectively.

The employed mechanism also reproduces the ratio of the K_L - K_S mass difference and the K_S width, by describing K_L as a bound state embedded in the $\pi\pi$ continuum. The model's results for $J^P = 1^+$ states containing one b quark are also discussed.

1 Introduction

Bound states embedded in the continuum have been suggested by von Neumann and Wigner [1]. Since then many works on this theme have appeared in various fields of physics [2–6]. In the

present paper, we shall study such states appearing as (approximate) solutions of our simple unitarised meson model [7]. As three concrete applications, we choose here the K_L - K_S system, the $D_{s1}(2536)$ [8] together with the very recently observed narrow $D_{sJ}^*(2463)$ [9,10] state, and finally the couple consisting of the established $D_1(2420)$ [8] and the preliminary broad $D_1(2400)$ [11,12] resonance. At first sight, it may seem odd to try to relate such utterly disparate states, ranging from mesons that can only decay weakly to very broad mesonic resonances. Moreover, while in the $J^P = 1^+ c\bar{n}$ (n stands for non-strange) system the $D_1(2400)$ is much broader than the slightly heavier $D_1(2420)$, for the $c\bar{s}$ states the likely $1^+ D_{sJ}^*(2463)$ is *even narrower* than the $1^+ D_{s1}(2536)$. Nevertheless, we shall demonstrate below that, in all three cases, a simple mechanism of coupling two degenerate $q\bar{q}$ channels with the same quantum numbers to the meson-meson continuum is capable of accounting for the experimental data, through an exact or approximate decoupling of one of the physical $q\bar{q}$ states.

2 Degeneracy lifting via coupling to the continuum

When two degenerate discrete channels are coupled to the same continuum channel, the degeneracy is lifted. One state decouples, partly or completely, depending on the details of the interaction dynamics, and turns into a continuum (approximate) bound state. The other state turns into either a resonance structure in the continuum, or a bound state below threshold when threshold is near enough. Within our unitarisation scheme, quark-antiquark channels are coupled to the meson-meson continuum by OZI-allowed 3P_0 $q\bar{q}$ pair creation and annihilation.

In the present investigation, we confine our attention to two degenerate quark-antiquark systems, which can be distinguished by some internal structure irrelevant for the coupling to the meson-meson continuum. For example, the constituent quark masses of u and d are the same in most models. Hence, the internal dynamics of $u\bar{u}$ and $d\bar{d}$ vector states can in meson models be described by the same Hamiltonian. Under $J^{PC} = 0^{++}$ quark-pair creation, both systems couple with the same intensity to pion pairs in P -wave. Nevertheless, because of the relative sign of the coupling constants under particle interchange [13], the $(u\bar{u} + d\bar{d})/\sqrt{2}$ state decouples from the two-pion continuum (ω meson), whereas the $(u\bar{u} - d\bar{d})/\sqrt{2}$ state decays strongly into pion pairs (ρ^0 meson).

Let us denote by ψ_1 and ψ_2 the wave functions of the quark-antiquark systems, and by H_1 and H_2 the Hamiltonians describing their internal confinement dynamics (*e.g.* employing a confinement potential). For the continuum we write the wave function ψ and the dynamics H . The coupling interactions of the two confinement channels to the continuum are denoted by V_1 and V_2 . In Ref. [13] it is found how the full spin, isospin and color degrees of freedom contribute

to the determination of such potentials. In the spirit of our model, we then obtain for the three channels the following set of coupled dynamical equations [14–17].

$$\begin{aligned}
(H - E) \psi + V_1 \psi_1 + V_2 \psi_2 &= 0 \\
V_1^\dagger \psi + (H_1 - E) \psi_1 &= 0 \\
V_2^\dagger \psi + (H_2 - E) \psi_2 &= 0 \quad .
\end{aligned} \tag{1}$$

We assume that the internal dynamics of the two degenerate quark-antiquark systems does not depend on the difference in their internal structure, and, moreover, that these systems also couple the same way to the continuum, i.e.,

$$H_1 = H_2 \quad \text{and} \quad V_1 = \alpha V \quad , \quad V_2 = \beta V \quad (\alpha^2 + \beta^2 = 1) . \tag{2}$$

In this case it is easy to sub-diagonalise the system (1), so as to obtain

$$\begin{aligned}
(H - E) \psi + V (\alpha \psi_1 + \beta \psi_2) &= 0 \\
V^\dagger \psi + (H_1 - E) (\alpha \psi_1 + \beta \psi_2) &= 0
\end{aligned} \tag{3}$$

and

$$(H_1 - E) (\beta \psi_1 - \alpha \psi_2) = 0 \quad . \tag{4}$$

We end up with a system of the continuum ψ coupled to a linear combination $\alpha \psi_1 + \beta \psi_2$ of the confinement states in Eq. (3), and with a completely decoupled system for the orthogonal linear combination $\beta \psi_1 - \alpha \psi_2$ in Eq. (4). Since, moreover, H_1 and H_2 are supposed to describe confinement, Eq. (4) has only bound-state solutions, all embedded in the meson-meson continuum.

3 The neutral kaon system

A typical example of the above-described phenomenon is the two-pion decay mode of the neutral kaon system. Both $d\bar{s}$ and $s\bar{d}$ couple weakly to $\pi\pi$ via the process depicted in Fig. 1. All other decay modes of neutral Kaons can to lowest order be neglected, since they couple orders of magnitude weaker.

Because of particle-antiparticle symmetry, we may assume $\alpha = \beta = 1/\sqrt{2}$. The $CP = -1$ combination $(d\bar{s} - s\bar{d})/\sqrt{2}$ completely decouples and turns into a bound state embedded in the $\pi\pi$ continuum. This combination thus represents the K_L meson, which, since CP violation is not contemplated in our model, has no coupling to the two-pion continuum. However, the

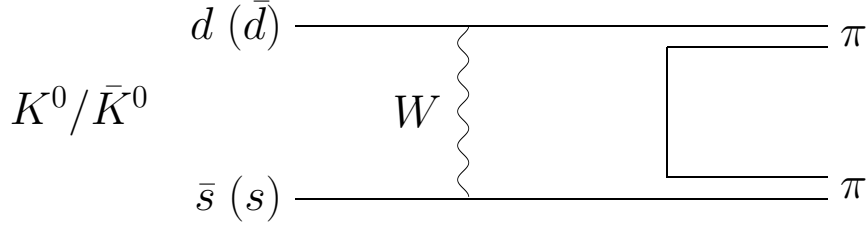


Figure 1: W exchange takes care of the flavour transitions triggering the strong process of quark-pair creation in weak K^0/\bar{K}^0 two-pion decay.

$CP=+1$ combination $(d\bar{s}+s\bar{d})/\sqrt{2}$ exists as a, actually extremely narrow, resonance in S -wave $\pi\pi$ scattering, hence describing the K_S meson.

We assume here that the decay process depicted in Fig. 1 is dominated by the strong OZI-allowed 3P_0 quark-pair-creation mechanism, whereas W exchange merely functions as a trigger to this process, which basically only determines the decay probability. Hence, besides the smallness of the parity-violating $K_S \rightarrow \pi\pi$ coupling constant, the transition potential describes here the coupling of a $u\bar{u}$ state with $J^{PC}=0^{++}$, i.e., σ -meson quantum numbers to two pions, similar to our unitarised description of scalar mesons studied in Refs. [14, 18, 19] (see also Ref. [20]). In the delta-shell approximation for the transition potential in the case of the scalar $K_0^*(800)$ and $a_0(980)$ resonances [18, 19], we obtained for the delta-shell radius a a value of about $a = 3.2$ GeV^{-1} . We shall hold on to this value in the following.

A general solution of Eq. (3) for the S -wave scattering phase shift $\cotg(\delta(s))$, as a function of the total invariant two-pion mass \sqrt{s} , is in this approximation and for small coupling given by

$$\cotg(\delta(s)) \approx \frac{\left[E_0 + R(s) |\mathcal{F}_0^{ds}|^2 \right] - \sqrt{s}}{I(s) |\mathcal{F}_0|^2} , \quad (5)$$

where E_0 represents the ground-state energy of the $d\bar{s}$ ($s\bar{d}$) when uncoupled, hence the mass of the K_L meson. The remaining factors $R(s)$, $I(s)$, and \mathcal{F}_0 are well explained in Ref. [21].

From expression (5) it is easy to perturbatively extract the real and imaginary part of the resonance pole position in the complex-energy plane, i.e.,

$$E_{\text{pole}} \approx E_0 + \Delta E , \quad \text{with} \quad \Re(\Delta E) = R(s) |\mathcal{F}_0|^2 \quad \text{and} \quad \Im(\Delta E) = I(s) |\mathcal{F}_0|^2 . \quad (6)$$

The position of the K_S resonance pole with respect to the K_L mass is shown in Fig. 2. Since the coupling of the neutral kaons to the two-pion continuum is extremely small, the arrow pointing from $\sqrt{s} = m_L$ to the K_S resonance pole position represents the pole trajectory for increasing intensity of the transition potential V_1 , too.

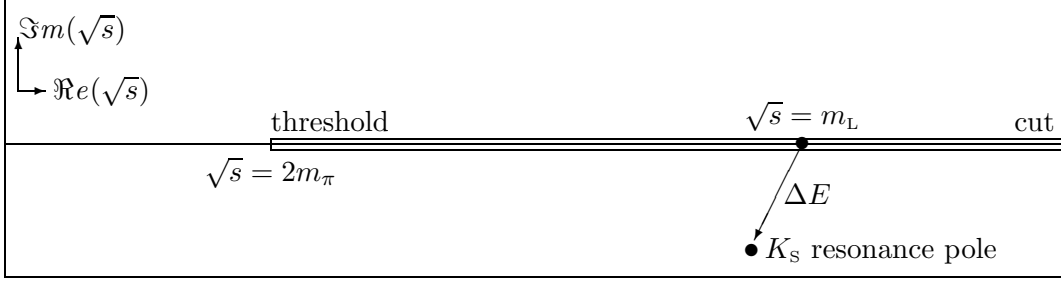


Figure 2: K_L bound-state pole embedded in the continuum, and K_S resonance pole in the second Riemann sheet.

For the ratio of the K_S decay width Γ_S , equalling twice the imaginary part (6) of the resonance pole position in the complex-energy plane, and the neutral-kaon mass difference, which equals the real shift (6) of the pole with respect to $E_0 = m_L$, we read from formula (5) the result

$$\frac{\frac{1}{2}\Gamma_S}{m_S - m_L} \approx \frac{I(s)}{R(s)} \quad . \quad (7)$$

From Ref. [21] we moreover learn that, in the case of S -wave scattering, one has

$$\frac{I(s)}{R(s)} = \frac{j_0(ka)}{n_0(ka)} = -\text{tg}(ka) \quad . \quad (8)$$

As a consequence of Eqs. (5), (7), and (8), we obtain an extremely simple relation for the mass difference in the neutral kaon system, the width of the K_S meson, the two-pion momentum k and the strong-interaction radius a , reading

$$\frac{\frac{1}{2}\Gamma_S}{m_L - m_S} \approx \text{tg}(ka) \quad . \quad (9)$$

Substitution of $k = 0.206 \text{ GeV}$ and $a = 3.2 \text{ GeV}^{-1}$ gives us then the result

$$\frac{\frac{1}{2}\Gamma_S}{m_L - m_S} \approx 1.3 \quad (\text{Experiment: } 1.06 \text{ [8]}) \quad . \quad (10)$$

Similar conclusions can be found in Refs. [22–26], where long-distance effects have been studied in more detail.

4 The $J^P = 1^+ \ c\bar{s}$ states

In the case of the $J^P = 1^+ \ c\bar{s}$ states, we deal with two distinct systems, 3P_1 and 1P_1 , which, as far as confinement is concerned, are degenerate when ignoring possible spin-orbit effects. Both states couple strongly to D^*K , with threshold at about 2.501 GeV.

For the neutral kaon system, we could straightforwardly assume that the transition potentials V_1 and V_2 in Eq. (1) are equal, because of particle-antiparticle symmetry. But for the $1^+ c\bar{s}$ systems we do not have such simple arguments. Nevertheless, if V_1 and V_2 are proportional, we still are in a situation comparable to the one discussed in the previous section, though now for strong interactions.

In Ref. [13] it is shown that the spatial form of the transition potential mainly depends on the orbital angular momenta of the $c\bar{s}$ and D^*K channels, whereas the relative intensities follow from recoupling coefficients. For transitions to vector+pseudoscalar we find that the intensity for 3P_1 is twice as large as for 1P_1 . Consequently, by the use of Eqs. (4) and (3), we conclude that the $J^P=1^+ c\bar{s}$ bound state embedded in the D^*K continuum consists of a mixture of 33% 3P_1 and 67% 1P_1 , whereas its supposed resonance partner has more or less the opposite content, but additionally with some D^*K admixture.

In Sec. (3) we have used Eq. (3) for the description of $\pi\pi$ scattering in the presence of the weak coupling to the neutral kaon system. Here, we assume that Eq. (3) is also suited to describe D^*K scattering in the presence of an infinity of $c\bar{s}$ confinement states. In our unitarised model, this just implies substituting the effective nonstrange quark mass by the charmed quark mass, the pion masses by the D^* and K masses, and changing some of the quantum numbers. The scattering phase shift is given by an expression similar to the one shown in Eq. (5), but, since the interaction is not weak now, also higher radial excitations of the $c\bar{s}$ confinement spectrum must be included. Thus, we use the general expression [14,18]

$$\cotg(\delta(s)) = \frac{n_0(pa)}{j_0(pa)} - \left[2\lambda^2 \mu p a j_0^2(pa) \sum_{n=0}^{\infty} \frac{|\mathcal{F}_n^{c\bar{s}}(a)|^2}{\sqrt{s} - E_n} \right]^{-1}. \quad (11)$$

Expression (11) is not only valid above threshold, where for small coupling ($\lambda \ll 1$) it generates Breit-Wigner-like resonance structures in the scattering cross section around each of the energy eigenvalues E_n ($n = 0, 1, 2, \dots$), but it is also valid below threshold. Resonances are characterized by complex-energy poles which are given by solutions of $\cotg(\delta(s)) = i$. When solutions of $\cotg(\delta(s)) = i$ come on the real-energy axis below threshold, then they describe the real energy eigenvalues for the bound state solutions of equation 3. For small values of λ the latter poles are found in the proximity of those E_n ($n = 0, 1, 2, \dots$) which come below threshold.

The non-relativistic form of the Flatté formula [27] can be obtained from formula (11) in the case of overlapping resonances. But, then its analytic continuation to below threshold is lost.

From expression (11) one can study the behavior of resonance poles, just being solutions of $\cotg(\delta(s)) = i$, in function of variations of the model parameters (see *e.g.* Ref [21]). Their passage from above threshold, where resonance poles exist in the the second Riemann sheet, to

below threshold, where poles are expected to reside on the real-energy axis in the first Riemann sheet, is smooth and without any difficulties. For S -wave scattering the ground-state pole hits the real-energy axis below threshold, then, for increasing values of λ , moves along the real-energy axis towards threshold where it changes Riemann sheet, turns 180 degrees and starts moving towards smaller values of energy.

Here, similarly to the procedure outlined in Ref. [14,18], we approximate the full sum over all $c\bar{s}$ confinement states by the two nearest states, that is, the ground state at E_0 and the first radial excitation at E_1 , plus a rest term. The latter is scaled to 1 by absorbing its value into the coupling constant λ , yielding

$$\sum_{n=0}^{\infty} \frac{|\mathcal{F}_n^{c\bar{s}}(a)|^2}{\sqrt{s} - E_n} \longrightarrow \frac{0.5}{\sqrt{s} - E_0} + \frac{0.2}{\sqrt{s} - E_1} - 1 \text{ GeV}^2 . \quad (12)$$

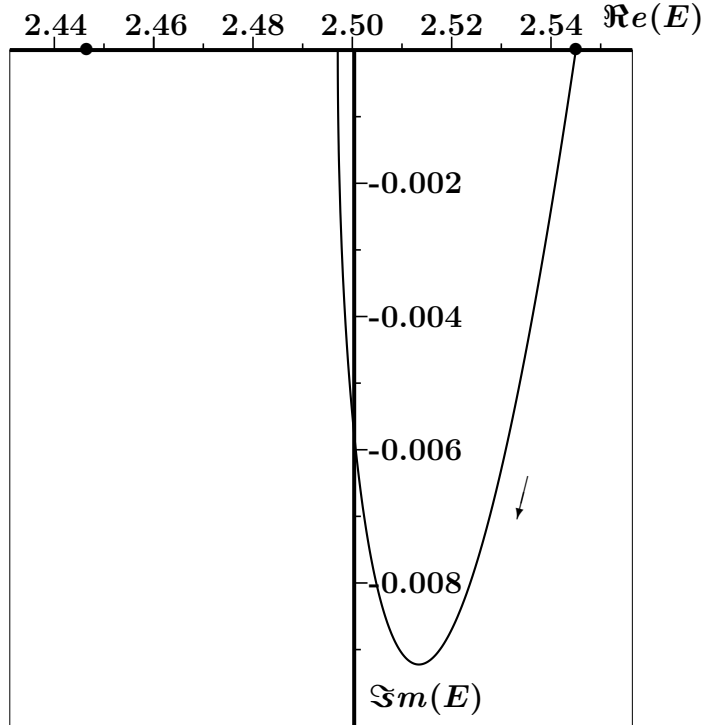


Figure 3: Trajectory of the ground-state pole in the D^*K scattering amplitude, as a function of the coupling constant λ , defined in Eq. (11), and which parametrises the intensity of the transitions between the pure $c\bar{s}$ system and the D^*K continuum (see Eq. 3). The arrow indicates how the pole moves when λ is increased. For vanishing coupling, as well as for the confined system described by Eq. (4), the pole is on the real E axis. For large coupling we find the pole on the real E axis below threshold. Units are in GeV.

We determine the ground-state mass of the uncoupled system (4) from the model parameters ($m_s = 0.508$, $m_c = 1.562$ and $\omega = 0.19$ GeV) given in Ref. [16], yielding $E_0 = 2.545$ GeV. This

also means that the bound state embedded in the D^*K continuum has exactly the mass E_0 , only 9 MeV away from the experimental $D_{s1}(2536)$ mass [8]. The first radial excitation lies $2\omega = 380$ MeV higher.

In Fig. 3 we study how the position of the ground-state singularity in the scattering amplitude for Eq. (3) varies, as the intensity of the transition potential V_1 is changed. In Nature one can only “measure” the pole position for one particular value of this intensity, given by strong interactions. Nevertheless, it is very illustrative to study alternative values. In particular, we notice that for larger intensities of the transition mechanism the pole comes out on the real E axis, below the D^*K threshold. Had we started from the perturbative formula (5), where $R(s)$ and $I(s)$ are proportional to λ^2 , we would have started out as in Fig. 2, and never returned to the real E axis for increasing values of the transition intensity. The trajectory in Fig. 3 is highly nonperturbative, which can only be achieved when all orders [21] are accounted for. The masses obtained for the model’s values of λ are indicated by \bullet in Fig. 3. For the $D_{sJ}^*(2463)$ we read from the figure $m = 2.446$ GeV, so, after all, this state is not a resonance as one would naively (i.e., perturbatively) expect from the coupled set of equations (3), in agreement with experiment. As mentioned above, for the $D_{s1}(2536)$ we obtain 2.545 GeV from pure confinement.

When the transition potentials V_1 and V_2 in Eq. (1) are not proportional, one has no simple diagonalisation, since commutators with the Hamiltonians will spoil the simplicity. Also, if H_1 and H_2 in Eq. (1) are not equal, diagonalisation will not lead to completely decoupled systems. However, from experiment we learn that the D^*K width of the $D_{s1}(2536)$ is small (less than 2.3 MeV [8]), implying that the bulk of the interaction indeed stems from the unitarisation mechanism.

5 The $J^P = 1^+$ $c\bar{n}$ states

In order to describe the ground states of the $J^P = 1^+$ $c\bar{n}$ spectrum, we use the same Eqs. (5) and (6) as in the previous case. Also here, we determine the ground-state mass of the uncoupled system (4) from the model parameters ($m_{u,d} = 0.406$, $m_c = 1.562$ and $\omega = 0.19$ GeV) in Ref. [16], which now yields $E_0 = 2.443$ GeV. Hence, the $J^P = 1^+$ $c\bar{n}$ bound state embedded in the $D^*\pi$ continuum comes out, in our model, at 2.443 GeV, some 20 MeV above the experimental [8, 11] $D_1(2420)$ mass. The first radial excitation lies, as before, $2\omega = 380$ MeV higher. The remaining parameters a and λ are kept the same as in the previous case, yet scaled with the reduced constituent $q\bar{q}$ mass $\mu_{q\bar{q}}$, in order to guarantee flavor invariance of strong interactions, *i.e.*

$$a_{xy} \sqrt{\mu_{xy}} = \text{constant} \quad \text{and} \quad \lambda_{xy} \sqrt{\mu_{xy}} = \text{constant} \quad , \quad (13)$$

where x and y represent the two flavors involved. The constants of formula (13) are fixed by [19] $a_{us} = 3.2 \text{ GeV}^{-1}$ and $\lambda_{us} = 0.75 \text{ GeV}^{-3/2}$ for S wave.

The resulting cross section is given in Fig. 4. Our peak shows up somewhat above 2.3 GeV, whereas the width of our $D_1(2420)$ is about 200 MeV. The corresponding experimental values are $2400 \pm 30 \pm 20 \text{ MeV}$ [11] ($2461^{+48}_{-42} \text{ MeV}$ [12]), and $380 \pm 100 \pm 100 \text{ MeV}$ [11] ($290^{+110}_{-90} \text{ MeV}$ [12]), respectively. In Fig. 4 we can further observe that the first radial excitation of the system

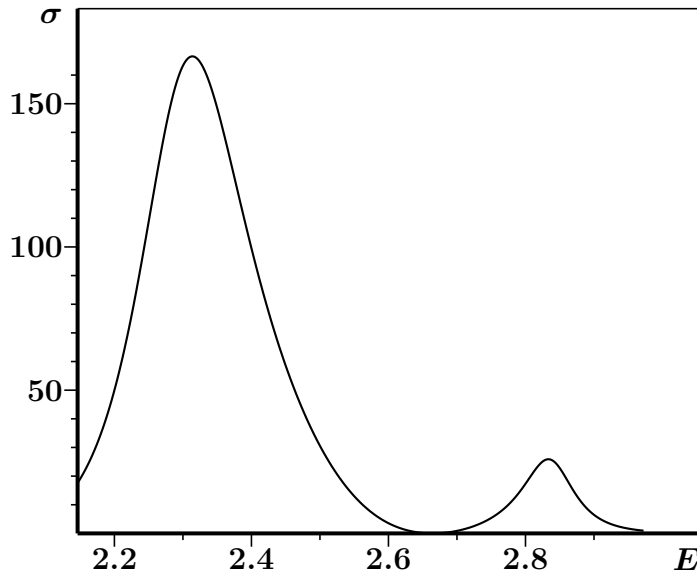


Figure 4: Model result for the cross section in units of GeV^{-2} for elastic S -wave $D^*\pi$ scattering, as a function of the total invariant mass E in units of GeV.

of equations (3), for $J^P = 1^+ c\bar{n}$, comes out more than 500 MeV higher than the ground-state resonance. Nevertheless, in expression (6) we always used $E_1 - E_0 = 380 \text{ MeV}$ [16]. Such a highly non-perturbative behaviour is inherent in the unitarisation procedure leading to formula (5).

The bound state $D_1(2420)$ embedded in the $D^*\pi$ continuum has zero width in our model, and so is invisible in the cross section of Fig. 4. On the other hand, experiment finds $18.9^{+4.6}_{-3.5} \text{ MeV}$ [8] and $26.7 \pm 3.1 \pm 2.2$ [11] MeV for the full width, which is nonetheless very small as compared to the available phase space. Consequently, also in this case our assumption in Eq. (2) appears to be reasonable.

The relative intensities α and β in Eq. (2) are the same as in the $c\bar{s}$ case. Hence, the relative content of the $D_1(2420)$ is again 33% 3P_1 and 67% 1P_1 . The $D_1(2400)$ roughly has the opposite mixture, plus a $D^*\pi$ component.

In Fig. 5 we show how the scattering pole moves in the complex-energy plane when λ is varied, which is the pole associated with the cross section of Fig. 4.

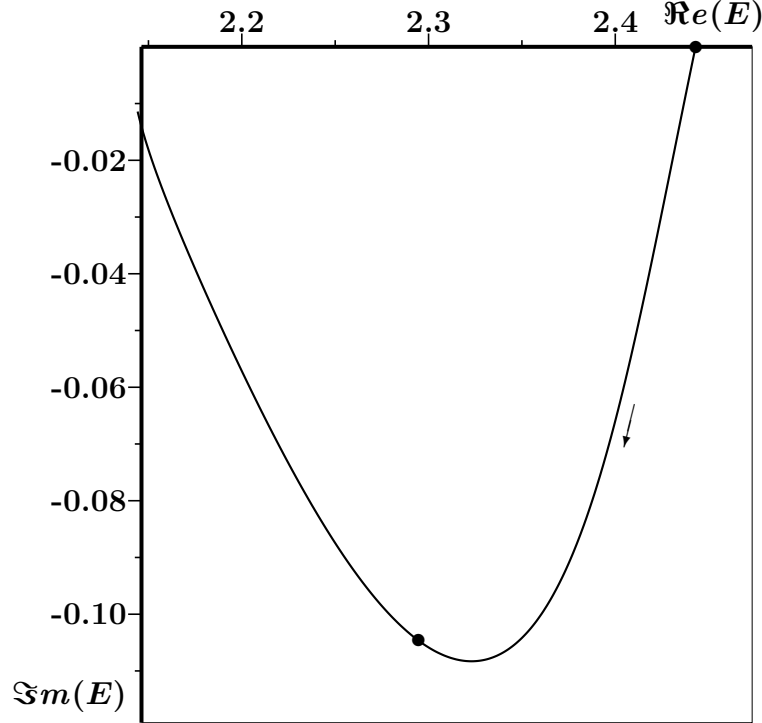


Figure 5: Trajectory of the ground-state pole in the $D^*\pi$ scattering amplitude, as a function of the coupling constant λ . The arrow indicates how the pole moves when λ is increased. For vanishing coupling, as well as for the confined system described by Eq. (4), here representing the $D_1(2420)$, the pole is on the real E axis. The pole position for Eq. (3), which describes the $D_1(2400)$, is indicated by \bullet for the physical value of λ . Units are in GeV.

6 $J^P = 1^+$ systems containing one b quark

For $J^P = 1^+$ systems containing one b quark we may repeat the above described procedure. We determine the ground-state masses of the uncoupled systems (4) from the model parameters ($m_{u,d} = 0.406$, $m_s = 0.508$, $m_c = 1.562$, $m_b = 4.724$ and $\omega = 0.19$ GeV) given in Ref. [16]. The remaining parameters a and λ are kept the same as for the case of the D mesons. This results in 5.707, 5.809 and 6.863 GeV for respectively $\bar{b}u/d$, $b\bar{s}$ and $\bar{b}c$. The model's results for the partner states which couple to the continuum, are collected in table (1). Similar to the case of $D^*\pi$ (section 5), we find in $B^*\pi$ a resonance structure above threshold, peak value at 5.6 GeV and some 120 MeV wide. The experimental result might be peaking at a slightly higher value [28–31], but the width of this resonance is in good agreement with our result. For the continuum bound state, which we find at 5.71 GeV, the OPAL collaboration reports a narrow resonance at 5.74 GeV [31], whereas the CDF collaboration gives 5.719 GeV for the narrow B_1 resonance [30]. We also might compare with the prediction of Kalashnikova and Nefediev, who obtain 5.716 and

5.741 GeV for the two B_1 states [32].

It should be noticed from table 1 that the $1^+ b\bar{s}$ partner state comes in our model at 5.73 GeV, which is in the same energy region as the other two states. However, the CDF collaboration reports a very small (3.7%) contamination due to B_s .

system	threshold GeV	continuum bound state GeV	partner state GeV	scattering length GeV ⁻¹
$\bar{b}u$	5.465 ($B^{*0}\pi^+$)	5.71	$5.59 - 0.06i$	-1.13
$b\bar{s}$	5.819 ($B^{*-}K^+$)	5.81	5.73	2.08
$\bar{b}c$	7.190 ($B^{*0}D^+$)	6.86	6.83	-31.8

Table 1: Purely bound states and partners for $J^P = 1^+$ systems containing one b quark.

Literally speaking, the $1^+ B_s$ and B_c do not make part of the combinations *continuum-bound-state/partner-state*, since even the purely bound states come below threshold. However, the case of $b\bar{s}$ could be different experimentally, given the error of some 10-30 MeV in our model predictions. So, there might be a continuum bound state, slightly above the B^*K threshold. But, the partner state is definitely below threshold and thus very narrow.

For B_c both states are well below threshold.

7 Summary and conclusions

In the present paper, we have studied examples of mesonic systems that generate bound or quasi-bound states in the continuum, within an unitarised quark-meson model. In the neutral-kaon system, our approach provides a simple explanation for the widths and the mass difference of the K_L and K_S , which is also in agreement with the conclusions of more sophisticated methods. Application to the $J^P = 1^+ c\bar{s}$ and $c\bar{n}$ axial-vector charmed mesons accomplishes a simultaneous description of the established narrow $D_{s1}(2536)$ and $D_1(2420)$ states, as well as the recently observed very narrow $D_{sJ}^*(2463)$, assuming it indeed is a 1^+ state, and broad $D_1(2400)$, which is rather problematic in standard quark models.

We predict the continuum bound states $D_1(2420)$ and $D_{s1}(2536)$ to be mixtures of 33% 3P_1 and 67% 1P_1 , which might be measured through radiative transitions [33]. For their partners $D_1(2400)$ and $D_{sJ}^*(2463)$ we predict more or less the opposite $^{2S+1}P_1$ -state content, but additionally with some $D^*\pi$ or D^*K admixture, respectively. This is in agreement with the mixtures proposed by

Godfrey and Kokoski in Ref. [34], based on the flux-tube-breaking mechanism. Their $\theta = -38^\circ$ for $c\bar{s}$ amounts to 38% 3P_1 and 62% 1P_1 regarding the state *degenerate* with 3P_2 , and the opposite content for the state *degenerate* with 3P_0 . The former mixture corresponds to the continuum bound state $D_{s1}(2536)$, which is indeed approximately degenerate with the 3P_2 in our model, since this $J=2$ state is subject to only very small unitarisation effects due to the D -wave D^*K channel. However, the latter mixture corresponds to the partner state D_{s1}^* at 2.443 GeV, which is strongly influenced by the coupling to the S -wave D^*K channel, just as the likely 3P_0 $D_{sJ}^*(2317)^+$ [35] is drastically affected by the S -wave DK threshold [36]. Therefore, no approximate degeneracy holds for these two charmed mesons. Concerning the $c\bar{u}$ states, Godfrey and Kokoski obtained $\theta = -26^\circ$, resulting in 19% 3P_1 and 81% 1P_1 , which indicates that our assumption (2) is probably somewhat less accurate in this case.

For $J^P = 1^+$ quark-antiquark systems which contain one b quark, we obtain good results as far as we can compare to experiment.

In conclusion, we have once again demonstrated that unitarisation has to be incorporated in realistic quark models of mesons and baryons, as it constitutes the second most important interaction after confinement.

Acknowledgements

This work was partly supported by the *Fundação para a Ciência e a Tecnologia* of the *Ministério da Ciência e do Ensino Superior* of Portugal, under contract number POCTI/FNU/49555/2002.

References

- [1] J. von Neumann and E. Wigner, Phys. Z. **30**, 465 (1929).
- [2] Lorenz S. Cederbaum, Ronald S. Friedman, Victor M. Ryaboy and Nimrod Moiseyev, Phys. Rev. Lett. **90**, 013001 (2003).
- [3] D. L. Pursey and T. A. Weber, prepared for *12th Int. Workshop on High-Energy Physics and Quantum Field theory (QFTHEP 97)*, Samara, Russia, 4-10 Sep 1997, published in *Samara 1997*, QFTHEP'97, pp. 435-438.
- [4] H. C. Rosu and J. Socorro, Nuovo Cim. B **113**, 677 (1998) [arXiv:gr-qc/9610018].
- [5] A. Khelashvili and N. Kiknadze, J. Phys. A **29**, 3209 (1996) [arXiv:quant-ph/9511022].

- [6] J. Pappademos, U. Sukhatme and A. Pagnamenta, Phys. Rev. A **48**, 3525 (1993) [arXiv:hep-ph/9305336].
- [7] Eef van Beveren and George Rupp, in Proc. Workshop *Recent Developments in Particle and Nuclear Physics, April 30, 2001, Coimbra (Portugal)*, (Universidade de Coimbra, 2003) ISBN 972-95630-3-9, pages 1–16, [arXiv:hep-ph/0201006].
- [8] K. Hagiwara *et al.* [Particle Data Group Collaboration], Phys. Rev. D **66**, 010001 (2002).
- [9] D. Besson [CLEO Collaboration], arXiv:hep-ex/0305100.
- [10] D. Besson *et al.* [CLEO Collaboration], to appear in Proc. *8th Conference on the Intersections of Particle and Nuclear Physics (CIPANP 2003), New York, 19-24 May 2003*, arXiv:hep-ex/0305017.
- [11] K. Abe *et al.* [BELLE Collaboration], BELLE-CONF-02-35, Cont. paper for the *31st Int. Conf. on High Energy Physics (ICHEP 2002), Amsterdam, The Netherlands, 24–31 Jul 2002*, session 8, *Heavy quark mesons and baryons (incl. lattice calculations)*, paper ABS724.
- [12] S. Anderson *et al.* [CLEO Collaboration], Conference report CLEO-CONF-99-6, (1999).
- [13] E. van Beveren, Z. Phys. **C21** (1984) 291.
- [14] Eef van Beveren and George Rupp, Talk given at *The 25th annual Montreal-Rochester-Syracuse-Toronto Conference on High-Energy Physics, Joefest, in the honor of the 65th birthday of Joseph Schechter, May 13 - 15, 2003, Syracuse (NY)*, to appear in AIP Conf. Proc. (2003), arXiv:hep-ph/0306155.
- [15] C. Dullemond, G. Rupp, T. A. Rijken, and E. van Beveren, Comput. Phys. Commun. **27** (1982) 377.
- [16] E. van Beveren, G. Rupp, T. A. Rijken, and C. Dullemond, Phys. Rev. D **27**, 1527 (1983).
- [17] E. van Beveren, C. Dullemond, and G. Rupp, Phys. Rev. **D21** (1980) 772 [Erratum-ibid. **D22** (1980) 787].
- [18] Eef van Beveren and George Rupp, Eur. Phys. J. C **22**, 493 (2001) [arXiv:hep-ex/0106077].
- [19] Eef van Beveren and George Rupp, AIP Conf. Proc. **619**, 209 (2002) [arXiv:hep-ph/0110156].
- [20] M. D. Scadron, Mod. Phys. Lett. A **14**, 1273 (1999) [arXiv:hep-ph/9910244].

- [21] E. van Beveren and G. Rupp, Int. J. Theor. Phys. Group Theor. Nonlin. Opt., in press (2003) arXiv:hep-ph/0304105.
- [22] G. E. Brown, J. W. Durso, M. B. Johnson and J. Speth, Phys. Lett. B **238**, 20 (1990).
- [23] I. I. Bigi and A. I. Sanda, Phys. Lett. B **148**, 205 (1984).
- [24] P. Cea and G. Nardulli, Phys. Lett. B **152**, 251 (1985).
- [25] John F. Donoghue, Eugene Golowich and Barry R. Holstein, Phys. Lett. B **135**, 481 (1984).
- [26] J. Lowe and M. D. Scadron, arXiv:hep-ph/0208118.
- [27] Stanley M. Flatté, Phys. Lett. B **63**, 224 (1976).
- [28] R. Barate *et al.* [ALEPH Collaboration], Phys. Lett. B **425**, 215 (1998).
- [29] M. Acciarri *et al.* [L3 Collaboration], Phys. Lett. B **465**, 323 (1999) [arXiv:hep-ex/9909018].
- [30] T. Affolder *et al.* [CDF Collaboration], Phys. Rev. D **64**, 072002 (2001).
- [31] K. Harder, arXiv:hep-ex/0110049.
- [32] Y. S. Kalashnikova and A. V. Nefediev, Phys. Lett. B **530**, 117 (2002) [arXiv:hep-ph/0112330].
- [33] Stephen Godfrey, arXiv:hep-ph/0305122.
- [34] Stephen Godfrey and Richard Kokoski, Phys. Rev. D **43**, 1679 (1991).
- [35] B. Aubert *et al.* [BABAR Collaboration], arXiv:hep-ex/0304021.
- [36] Eef van Beveren and George Rupp, arXiv:hep-ph/0305035.